26th ABCM International Congress of Mechanical Engineering
November 22-26, 2021. Florianópolis, SC, Brazil

Wax Deposition Experiment Under Cold Flow: A Transient Analysis

Alexandre Martins
Antonio C. Bannwart
School of Mechanical Engineering - University of Campinas. Campinas, São Paulo, Brazil
alexandremartins30@msn.com
bannwart@fem.unicamp.br

Ivanei F. Pinheiro
Leticia Bizarre
Charlie Van Der Geest
Vanessa C. B. Guersoni
Center for Petroleum studies, University of Campinas, Campinas, São Paulo, Brazil
ivanei@unicamp.br
lbizarre@unicamp.br
geest@unicamp.br
vanessa@cepetro.unicamp.br

Abstract. *The Wax deposition is one of the biggest flow assurance problems when producing waxy crude oils, and because it is not completely understood, still contains several aspects that need further investigation for a better comprehension of the phenomenon. When the temperature of the bulk is above the Wax Appearance Temperature, i.e. hot flow, there is a lot of disagreement in the literature regarding the causation between the final thickness (steady-state) and the thermal driving force, a more accurate way to correlate both is to use the dimensionless temperature difference. However, for the cold flow, the trend is better understood, the literature evidence shows that the final wax thickness is proportional to the thermal driving force. It is interesting to point out that the majority of experiments that observed those behaviours were executed with model oil. The first step of this research was to evaluate whether the same behavior occurs for Brazilian waxy crude oil under cold flow conditions. This work reports an experimental wax deposition study under cold flow conditions and varying conditions of temperature and flow rate to observe their influence on wax deposition rate. The wax deposition thickness was calculated using the pressure drop method. Another interesting analysis done in this research is the time necessary to reach steady-state by measuring the bulk temperature gradient, as the deposit increases, the temperature gradient between the inlet and outlet decreases, evidence that the energy being transferred from the oil to the coolant reduces as the deposit grows. Therefore, this is an easy methodology to investigate the transient time of the wax deposition, which could help the definition of PIG (Pipeline Inspection Gauge) frequencies during production and improving both in reducing costs and stops in oil production.*

Keywords: *Flow Assurance, Wax Deposition, Waxy Crude Oil, Thermal Driving Force*

1. INTRODUCTION

In a sub-sea oil production systems, pipelines are exposed to very low temperatures, there is no economically viable method to isolate the pipelines to decrease heat exchange between internal fluid flow and external environment in order to avoid flow assurance problems. As the temperature of the oil goes down, the solubility of wax in the oil decreases, until it reaches the wax appearance temperature (WAT), causing the precipitation of wax crystals that form deposits in the inner walls of pipelines (Azevedo and Teixeira, 2003; Mehrotra *et al.*, 2020). These deposits can partially obstruct or totally block the pipeline, leading to a series of operational problems. Several studies have been conducted to quantify wax deposition, but the proposed models are incapable of accurately predicting the deposition due to the complexity of the mechanisms involved in the phenomenon (Van Der Geest *et al.*, 2021).

Burger *et al.* (1981) argued in their work that the most relevant mechanism of wax deposition is the molecular diffusion. A radial concentration gradient induces the transportation of the wax molecules from the bulk to the pipe wall (Van Der Geest *et al.*, 2018). It is a concept that is widely used until today, with models that accomplished reasonably good results in predicting wax deposition by tuning parameters, Singh *et al.* (2000) and Matzain (1996) are examples.

According to Soedarmo *et al.* (2016), in turbulent flows, models purely based on molecular diffusion tend to overpredict the deposition, and a concept that is commonly assumed is that a shear stripping mechanism is acting in the deposit. A

partial removal of the deposit as a result of the shear effect, several authors (Correra *et al.*, 2007; Matzain, 1996; Venkatesan, 2004) developed semi-empirical models in order to take these effect into account. It is important to highlight that the shear stripping effect has never been experimentally isolated and confirmed.

Besides the commonly used mass transfer approach, there is a different approach to model wax deposition, which is the phase transition approach. This approach can predict some behaviours observed in experiments that the mass transfer approach cannot, e.g. the decrease of the deposit as Reynolds number increase. The main hypothesis of this approach is that the formation of the deposit is a thermodynamic process of phase transition, what limits the growth is the amount of heat being removed from the bulk, as the deposit grows, the rate of heat being transferred decreases, once this is not enough to overcome the latent heat of solidification, the deposit stops to increase (Mehrotra *et al.*, 2020).

Regardless of the discussion of what is the principal mechanisms, the thermal driving force is an important variable for both approaches, thus wax deposition can be investigated by the difference between the temperature inside the pipeline and the temperature outside the pipeline. In this research we define them as the oil temperature ($\bar{T}_{bulk}$) and the coolant temperature ($T_{coolant}$), and the goal is to understand how that influences the wax deposition thickness.

Bidmus and Mehrotra (2009) conducted an experimental investigation to study wax deposition in a flow-loop apparatus. They performed experiments using two different concentrations of wax-solvent mixtures under both cold ($\bar{T}_{bulk} < WAT$) and hot flow ($\bar{T}_{bulk} > WAT$) regimes. They analyzed the deposition data with a steady-state heat transfer model and confirmed that the deposition process was thermally driven. During cold flow, they observed that the deposit mass decreases with the increase of the coolant temperature and with the decrease of the temperature wax-solvent mixture. The Reynolds number did not affect the deposit mass, and as expected, greater concentration of wax result in greater deposit mass. They argued that the thermal driving force, defined as $T_{bulk} - T_{coolant}$, is not the best parameter to understand tendencies on wax deposition, the best being the dimensionless temperature, defined as $\theta_d = \frac{T_{int} - T_{coolant}}{T_{bulk} - T_{coolant}}$.

Another interesting work that studies this issue is from Arumugam *et al.* (2013), they developed a model applicable to both cold and hot flow using a correlation for the wax precipitation temperature (WPT) as a function of the wax concentration and the cooling rate, this way they could predict the transition between cold and hot flow regime. Their results appointed that under cold flow regime the predicted deposit thickness tends to decrease, in hot flow it tends to increase and the maximum deposit prediction occurred in the transitional region.

In this work, we intend to do an analyses in wax deposition using waxy crude oil flowing in a flow-loop apparatus. The experiments reported in literature were majority done with model oil, the intention of this work is to evaluate the influence of thermal driving force and dimensionless temperature difference doing experiments with real oil. During this test campaign, only experiments in cold flow regime were executed due to the experimental apparatus limitations.

2. METHODOLOGY

In the study reported in this paper, a series of experiments were performed under cold flow conditions in a flow-loop apparatus using a Brazilian waxy crude oil.

2.1 Densimeter

The oil density was measured using an Anton Paar DMA 4500 densimeter. The process consists in using a syringe to insert the sample into the measuring cell until its entire volume was completely. The density measurements were performed at temperatures from 60 to 4 ° C.

2.2 Rheometer

The equipment used for all rheological analyses was the Thermo Scientific HAAKE Mars III stress-controlled rheometer using a cone and plate geometry with 60 mm diameter and a cone angle of 1 degree with truncation of 0.052 mm also using a Peltier plate, the gap was controlled using the thermo-gap option. An experiment was done to evaluate the influence of temperature on the behavior of the oil, the experiment consists of varying the temperature from 70 °C to 5 °C, applying a shear rate throughout the procedure. Each sample was kept 70 °C for at least 2 hours for removing any history. After that, the samples were added to the rheometer and homogenized for 10 minutes at 70 $^{\circ}C$ with a shear rate of 10 s^{-1}. After that, the measurement started.

2.3 Differential Scanning Calorimetry (DSC)

The wax appearance temperature (WAT) was determined using a calorimeter (Q2000, TA Instruments). Initially the samples were heated from 40 to 80°C under a nitrogen atmosphere and kept at 80°C for 10 minutes to erase the thermal history of the sample.The sample was then cooled to -30°C at a rate of 3°C/min

2.4 Flow-Loop Apparatus.

The layout of the flow loop experiment is shown in Figure 1. The waxy crude oil is pumped through the steel pipes, shown in red, until the test section, shown in blue, from the test section, it returns to the tank. The tank is heated, enabling the control of the oil temperature. The test section pipeline has diameter of 1 inch and 3.5 m of length, and it is made of copper, which has a higher thermal conductivity. The test section stays inside a water bath, which is represented by the box around the blue pipeline. The water temperature can be controlled in a range from 70 to 5 °C. About the instrumentation, the flow-loop has one pressure gauge (Rosemount 2088 with accuracy ±0.05 bar) in the inlet of the test section, and a differential pressure gauge (Rosemount 3051 with accuracy ± 2.5 mbar) in the test section, with a length of 1.68 m. For temperature measurement, 3 four-wire PT-100 sensor (accuracy ± 1 °C) were used, one at the inlet and another at the outlet of the test section (these are measuring oil temperature). The last sensor is installed inside the water bath, the temperature and volumetric flow rate of the water are controlled.

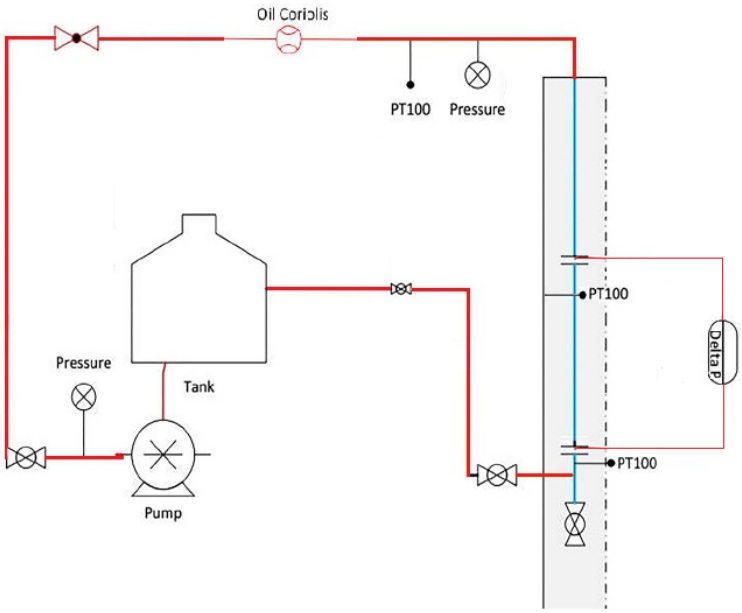

Figure 1: Layout of the experiment apparatus.

During the experiments, the wall pipeline temperature it is not measured, heat transfer models were used to obtain this value.

2.4.1 Experimental Matrix.

The experimental matrix is shown in Table 1. It was performed a total of nine tests, with a running time of approximately 110 hours. The first five tests were to investigate the influence of the oil flow rate, in sequence, it was performed two tests varying the coolant temperature, the last two tests were done to evaluate the influence of bulk temperature. The experimental data shown in Table 1 is composed of the average values during each test.

Table 1: Experimental Matrix

Test	**Duration time (h)**	$T_{bulk_{in}}$ **(°C)**	$T_{bulk_{out}}$ **(°C)**	$T_{coolant}$ **(°C)**	Q_{bulk} (m³/h)
1	110.8	39.8	39.4	5	3.8
2	110.3	40.0	39.4	5	5.0
3	110.7	40.1	39.7	5	6.3
4	110.7	40.3	39.9	5	7.5
5	111.1	40.4	40.1	5	8.7
6	111.3	40.0	39.4	15	5.0
7	111.3	40.1	39.8	25	5.0
8	111.7	45.1	44.8	5	6.5
9	109.5	49.9	49.3	5	6.7

3. RESULTS AND DISCUSSION

3.1 Oil Properties

Applying the least square method to the density measurements, the best fitted equation was used to calculate the average density during the experiments, the result is shown in Figure 2a. The viscosity fit was done for temperatures ranging from 40°C to 50°C, because of experimental matrix, as discussed before. Figure 2b shows the best viscosity fit for the oil used in the experiments.

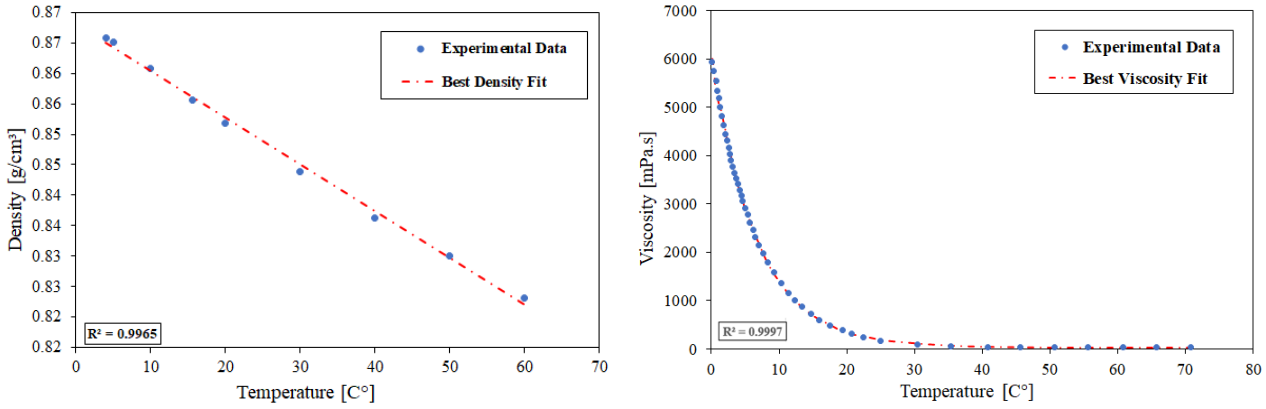

(a) (b)

Figure 2: (a) Density of the crude oil varying with temperature and (b) viscosity of the oil sample from 70 to 5 °C.

3.1.1 DSC

The cooling thermogram is shown in Figure 3, this curve shows two peaks characteristic of paraffin oil, that confirm the crystallization of micro and macro wax crystals respectively around 50°C and 25°C (Kurniawan *et al.* (2018)). Micro wax crystals are formed by branched and cyclic alkanes, so it has higher molecular weight and therefore crystallizes at higher temperatures than macro wax Japper-Jaafar *et al.* (2016). Macro-paraffin crystals are formed by n-alkanes with a lower molar mass than micro-paraffins and tend to form large crystals near room temperature (second peak).

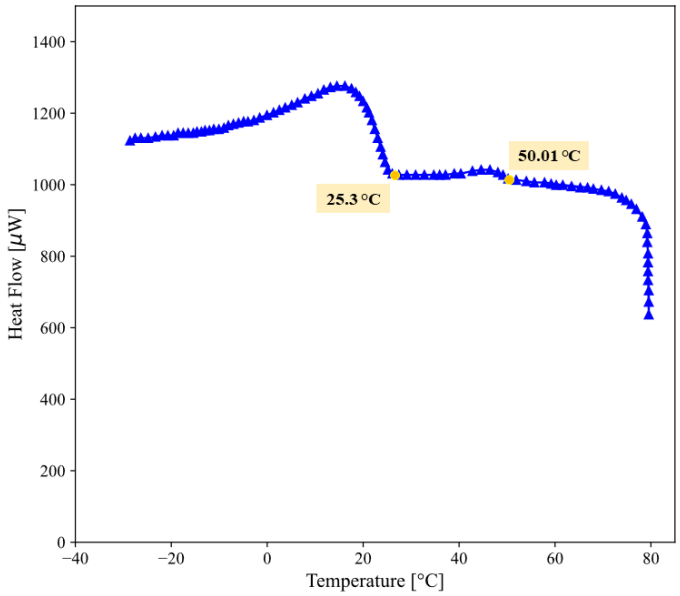

Figure 3: Thermogram of the oil sample measured by DSC method for a cooling rate of -3°C/min.

3.2 Theoretical Background

3.2.1 Fluid Mechanics.

All results obtained from the experiments were calculated assuming constant radial viscosity and fully develop flow, according to White (2011) for horizontal incompressible flow we can simplify the energy conservation. The test section is a strait pipeline with no local losses, therefore we can just consider the classical analytical solution for laminar and the classic Blassius equation for smooth pipelines for turbulent flow.

$$\frac{\Delta P}{\rho g} = f\frac{L}{D_w}\frac{V^2}{2g} \qquad \longrightarrow \qquad f = \begin{cases} \frac{64}{Re} & \longrightarrow Re < 2000 \\ 0.316Re^{-1/4} & \longrightarrow Re > 2000 \end{cases} \tag{1}$$

where ΔP is the differential pressure, ρ is the density, g is the gravity, f is the friction factor, L is the length, D_w is the inner wall pipeline diameter, V is the fluid velocity and Re is the Reynolds number.

3.2.2 Steady State Heat Transfer.

For the heat transfer calculation it is important to highlight that this paper only does steady state calculations. Even though we show transient results, the heat transfer model is just a guide to understand the influence between coolant and bulk temperatures. The equation for the total heat transfer coefficient (U_{tot}) (Davenport and Conti, 1971), was used to estimate the temperature distribution once steady state was reached. Assuming that the length is order of magnitude bigger than the diameter, thus the variation of the diameter in the area through which heat is transferred is negligible, e.g. oil-deposit interface area (A_{int}) $\approx$ pipeline wall area (A_{wall}) meaning that for the overall heat transfer calculation, all diameters are the same.

$$q = U_{tot}A_{int}(T_{\infty oil} - T_{\infty water}) \qquad \longrightarrow \qquad \frac{1}{U_{tot}} = \frac{1}{h_{oil}} + \frac{D_{int}ln(\frac{D_w}{D_{int}})}{2k_{deposit}} + \frac{D_{int}ln(\frac{D_o}{D_w})}{2k_{pipeline}} + \frac{1}{h_{water}} \tag{2}$$

where $T_{\infty oil}$ is the temperature of the bulk of the oil, $T_{\infty water}$ is the temperature of the water away from the wall, h_{oil} is the oil heat transfer coefficient, D_{int} is the diameter until the interface of the deposit, D_o is the outside diameter of the pipeline, $k_{deposit}$ and $k_{pipeline}$ are the thermal conductivity of the deposit and the copper respectively, and h_{water} is the water heat transfer coefficient. For more detailed information about Eq. 2 see Eq. 6 and Eq. 7 in the Appendix section.

In this paper, the goal is not to discuss in detail heat transfer analysis neither to discuss the models, it is rather an analysis of the general behaviour and tendencies based on the dimensionless temperature difference, and to show further evidence that the deposit works as an isolation layer as the thickness increase.

It is important to highlight that as the wax precipitates, the crude composition changes, which means that the WAT of the bulk decreases as the wax precipitate. In this paper, WAT always refers to the original crude oil, before any precipitation event. In a cold flow, the bulk is below WAT, thus in all experiments, the crude oil in the bulk is not the same as the original, because wax has precipitated. Thus, T_{int} is always below WAT (original crude WAT).

$$T_{int} = T_{\infty oil} - \frac{U_{tot}}{h_{oil}}(T_{\infty oil} - T_{\infty water}) \qquad \longrightarrow \qquad T_{wall_{in}} = T_{int} - \frac{U_{tot}}{\frac{2k_{deposit}}{D_{int}\ln\left(\frac{D_w}{D_{int}}\right)}}(T_{\infty oil} - T_{\infty water}) \tag{3}$$

$$\theta_d = \frac{T_{int} - T_{wall_{in}}}{T_{bulk} - T_{coolant}} \tag{4}$$

where T_{int} is the average temperature at oil-deposit interface, $T_{wall_{in}}$ is the average temperature at the pipeline inside wall, $T_{coolant}$ is the average temperature of the coolant, T_{bulk} is the average temperature of the bulk and θ_d is the dimensionless radial temperature difference. For more detailed information about Eq. 4 see Eq. 8 and Eq. 9 in the Appendix section.

3.2.3 Wax Thickness Calculation.

In this work the method used to calculate the wax thickness is the pressure drop method, this methodology is already well-known and used in another studies (Van Der Geest *et al.*, 2018; Hoffmann and Amundsen, 2010; Panacharoensawad and Sarica, 2013; Yang *et al.*, 2020). An algorithm was programmed for receive the data measured from the flow-loop acquisition system, it first converts the selected parameters data trends in average values, next an average value for density and viscosity is calculated using the data experimental data fit obtained from the laboratory measures in order to calculate

Reynolds, friction factor and shear stress for each experiment, finally it obtains the wax deposition thickness solving Equation 3.

$$F(\delta) = \frac{(\frac{dP}{dL})|_t}{(\frac{dP}{dL})|_0} - \frac{(\frac{fV^2}{d})|_t}{(\frac{fV^2}{D_w})|_0} \simeq 0 \tag{5}$$

The pressure drops throughout the experiments are known, as are the pressure drop and the pipeline diameter at the start of the experiment. Considering the pressure drop and friction factor at time 0 as parameters of normalization, the algorithm could solve Equation 3 using the Newton-Raphson method. This equation is dependent on the diameter changes, which in turn is dependent on the friction factor and the fluid velocity.

It is important to emphasize that in this experiments was assumed that all the variation in the pressure drop profile is due to diameter variation, this is clear since it was used the pressure drop at the beginning of the experiment to define the pressure drop. The only way to verify our calculated experimental wax thickness is by measuring the weight of wax in the pipeline, which was not possible during this test campaign. That has already been solved, further studies will have two removable sections.

3.3 Main Results

We will start this discussion by analyzing each comparison done with the wax deposition thickness calculated using the pressure drop method. The first behavior that is noted in all the experiments results is the tendency of the curves to increase and decrease in time, revealing a pattern in all tests. This behavior is due to difficulties in the temperature control. It is possible to see that approximately at every 24 hours the wax deposition thickness curves complete one “period”, that is because of the differences of ambient temperature between day and night. The temperature sensor that control the water temperature is several meters away from the test section, thus during the night time, the temperature in the test section drops by up to $0.8°C$ which affect the viscosity of the fluid, as the flow rate rises, the pressure drop also rises, thus the influence of this small variation in the water temperature becomes smaller.

After explaining the oscillation due to difficulties in controlling the water temperature, we can start to analyze the influence of the oil flow rate in the wax thickness. Figure 4 shows a comparison between calculated wax thickness during the experiments in different flow rates, to isolate this effect we maintained the temperatures of water and bulk constant. It is possible to observe that as the flow rate increases the deposition thickness decreases for cold flow conditions, that is a behavior that is well-establish in literature (Cabanillas *et al.*, 2016; Singh *et al.*, 2000). This can be explained by simple heat transfer analysis. As the flow rate increases, so does the heat transfer, increasing the temperature of the wall , and consequently decreasing the size of the deposit (Mehrotra *et al.*, 2020; Van Der Geest *et al.*, 2021).

Figure 4 also shows that as the flow rate increases the time to measure an increase in wax thickness also increases, a delay of around 10 hours occurred for the biggest flow rate (Re = 4440.2), this needs to be further investigated, because it is close to the pressure drop sensor errors.

Figure 5 shows a comparison between calculated wax thickness during the experiments at the same flow rate of Re = 2500 at constant bulk temperature of 40° C. Here we are evaluating how the coolant temperature influences in the final wax thickness, as the coolant temperature increases the thermal driving force decreases and also the wax thickness, which means in this case the thermal driving force could be considered a parameter that directly influences the wax deposition thickness. The fact that the increase of the coolant temperature result in the decrease of the deposit thickness was already showed in early studies, as in the work of Bidmus and Mehrotra (2009).

Figure 6 shows a comparison between calculated wax thickness during the experiments at the same flow rate of approximately 6.5 m³/h and constant coolant temperature of 5° C. Here we are evaluating how the bulk temperature influences in the final wax thickness, as the bulk temperature increases from 40 °C to 45°C the thermal driving force increases and also the wax thickness. When the bulk temperature increases from 45 °C to 50°C the thermal driving force increases but the wax thickness decreases. Both pipe wall and bulk temperature seems to be unrelated to the final wax thickness in this case. The incoherence in these results needs further investigation, because there are experimental results in the literature that argue that when the oil is close to the WAT, it is when the thickness shall be the biggest. All this analyses are hypotheses we could try to investigate in the future.

Figures 7a and 7b show the inlet and outlet temperature trends for experiments at the same flow rate of 5 m³/h, the constant bulk temperature of 40° C and coolant temperature of 5° C and 25° C respectively. It is possible to see that in these two experiments the inlet and outlet oil temperatures tend to approach each other over time, we saw this behavior in most of the tests we performed. This is clear evidence that the wax deposit layer acts as thermal insulator, causing the energy transferred from the oil to the coolant to decrease. This is also a possible methodology to obtain the transient time of the phenomena. Once the temperature gradient between the inlet and the outlet becomes constant, the steady state regime has been reached and theoretically, the deposit shall stop growing.

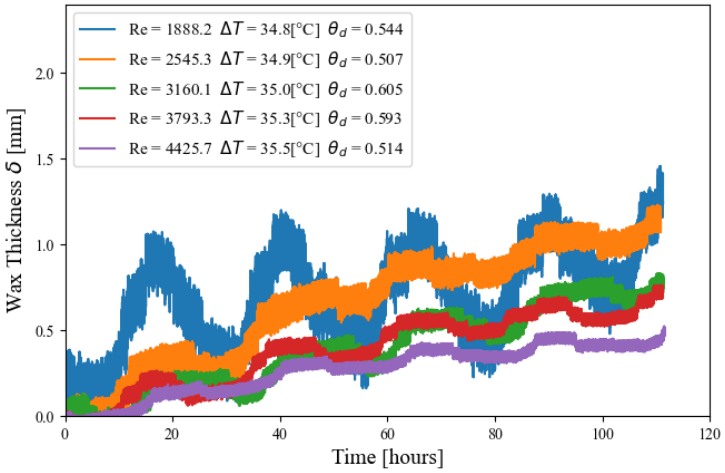

Figure 4: Comparison of wax deposit thickness buildup in time for different oil flow rates with $T_{bulk} \simeq 40$ °C and $T_{coolant} \simeq 5$ °C. ΔT is the average thermal driving force and θ_d is the dimensionless radial temperature difference for the wax deposition final thickness.

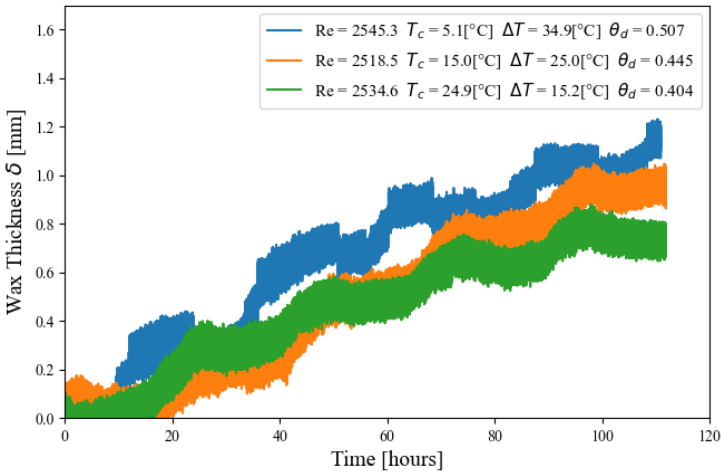

Figure 5: Comparison of wax deposit thickness buildup in time for different coolant temperatures (T_c) with $Q_{bulk} \simeq 5.0$ m³/h and $T_{bulk} \simeq 40$ °C.

4. CONCLUSION

An analysis about wax deposition was conducted with the main objective of investigating the influence of the thermal driving force in an experiment using waxy crude oil. We observed that with the increase of the flow rate, and consequently of the Reynolds number, the final wax thickness was reduced, which can be easily explained by an heat transfer analysis. When we maintain the temperature of the oil constant and increase the coolant temperature, the thickness decreases, which is in agreement with the literature. It can be said that the thermal driving force is not the best method to correlate with the deposit thickness, begin the dimensionless temperature a better approach.

In all experiments there is clear evidence that the deposited layer is acting as a thermal insulator, there is a transient period where for a constant inlet temperature, the outlet temperatures increases until reaching an asymptote, which indicated that the steady state has been reached. This shall be used in future experiments to determine when we shall stop the experiment and to verify whether or not the aging process influences the heat transfer.

5. ACKNOWLEDGEMENTS

We would like to thank ANP (National Agency of Petroleum, Natural Gas and Biofuels). We would also like to thank the School of Mechanical Engineering (FEM) and the Center for Petroleum Studies (CEPETRO) at the University of Campinas (UNICAMP). Acknowledgments are also extended to ALFA research group for their support.

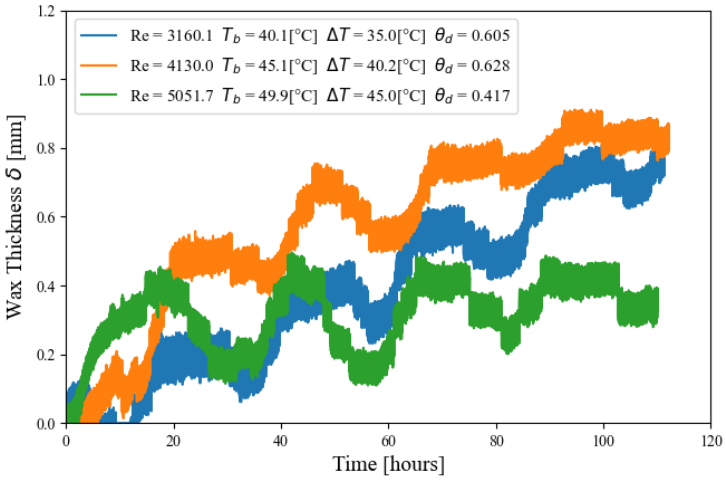

Figure 6: Comparison of wax deposit thickness buildup in time for different bulk temperatures (T_b) with $Q_{bulk} \simeq 6.5$ m³/h and $T_{coolant} \simeq 5$ °C.

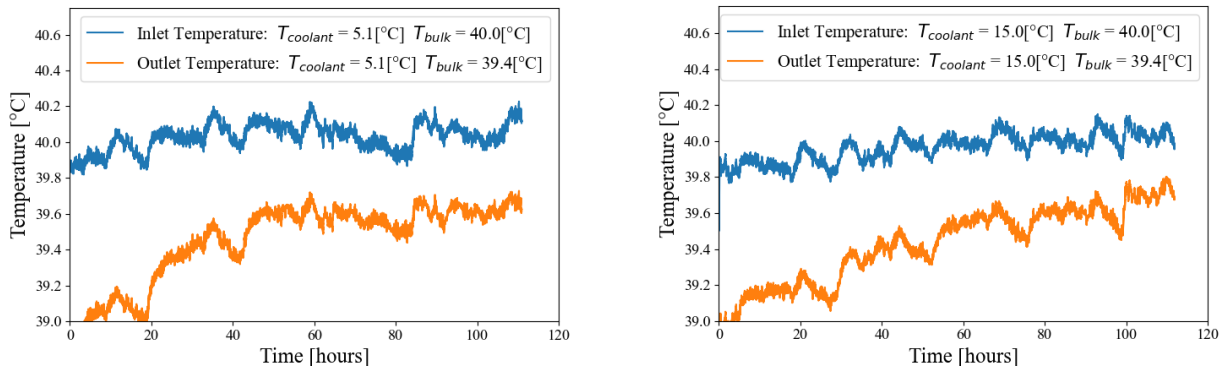

(a) (b)

Figure 7: Experimental data of inlet and outlet temperature representing the isolation effect of the wax layer: (a) $Q_{bulk} \simeq 5.0$ m³/h and $\Delta T \simeq 35$ °C and (b) $Q_{bulk} \simeq 5.0$ m³/h and $\Delta T \simeq 15$ °C.

6. REFERENCES

Arumugam, S., Kasumu, A.S. and Mehrotra, A.K., 2013. "Modeling of solids deposition from "waxy" mixtures in "hot flow" and "cold flow" regimes in a pipeline operating under turbulent flow". *Energy Fuels*, Vol. 27, pp. 6477–6490.

Azevedo, L.F.A. and Teixeira, A.M., 2003. "A critical review of the modeling of wax deposition mechanisms". *Petroleum Science and Technology*, Vol. 21:3, pp. 393–408.

Bidmus, H.O. and Mehrotra, A.K., 2009. "Solids deposition during "cold flow" of wax-solvent mixtures in a flow-loop apparatus with heat transfer". *Energy Fuels*, Vol. 23, pp. 3184–3194.

Burger, E.D., Perkins, T.K. and Striegler, J.H., 1981. "Studies of wax deposition in the trans alaska pipeline". *Journal Of Petroleum Technology*, pp. 1075–1086.

Cabanillas, J.P., Leiroz, A.T. and Azevedo, F.A., 2016. "Wax deposition in the presence of suspended crystals". *Energy Fuels*, Vol. 30, pp. 1–11.

Correra, S., Fasano, A., Fusi, L. and Merino-Garcia, D., 2007. "Calculating deposit formation in the pipelining of waxy crude oils". *Meccanica*, Vol. 42, pp. 149–165.

Davenport, T.C. and Conti, V.J., 1971. "Heat transfer problems encountered in the handling of waxy crude oils in large pipelines". *Journal of the Institute of Petroleum*, Vol. 57(555), p. 147.

Hoffmann, R. and Amundsen, L., 2010. "Single-phase wax deposition experiments". *Energy Fuels*, Vol. 24, pp. 1069–1080.

Japper-Jaafar, A., Bhaskorob, P.T. and Miorc, Z., 2016. "A new perspective on the measurements of wax appearance temperature: Comparison between dsc, thermomicroscopy and rheometry and the cooling rate effects." *Journal of Petroleum Science and Engineering*, Vol. 147, No. –, pp. 672—-681.

Kurniawan, M., Subramanian, S., Norrman, J. and Paso, K., 2018. "Influence of microcrystalline wax on the properties of model wax-oil gels". *Energy & Fuels*, Vol. 32, No. 5, pp. 5857–5867.

Matzain, A., 1996. *Single Phase Liquid Paraffin Deposition Modeling*. Master's thesis, The University of Tulsa, Tulsa, OK.

Mehrotra, A.K., Ehsani, S., Haj-Shafiei, S. and Kasumu, A.S., 2020. "A review of heat-transfer mechanism for solid deposition from "waxy" or paraffinic mixtures". *The Canadian Journal of Chemical Engineering*, Vol. 98, No. 12, pp. 2463–2488.

Panacharoensawad, E. and Sarica, C., 2013. "Experimental study of single-phase and two-phase water-in-crude-oil dispersed flow wax deposition in a mini pilot-scale flow loop". *Energy Fuels*, Vol. 27(9), pp. 5036–5053.

Singh, P., Venkatesan, R., Fogler, H.S. and Nagarajan, N., 2000. "Formation and aging of incipient thin film wax-oil gels". *AIChE Journal*, Vol. 46(5), pp. 1059–1074.

Soedarmo, A.A., Daraboina, N. and Sarica, C., 2016. "Microscopic study of wax deposition: Mass transfer boundary layer and deposit morphology". *Energy Fuels*, Vol. 30, pp. 2674–2686.

Van Der Geest, C., Guersoni, V.C.B., Merino-Garcia, D. and Bannwart, A.C., 2018. "Wax deposition experiment with highly paraffinic crude oil in laminar single-phase flow unpredictable by molecular diffusion mechanism". *Energy & Fuels*, Vol. 32, No. 3, pp. 3406–3419.

Van Der Geest, C., Melchuna, A., Bizarre, L., Bannwart, A.C. and Guersoni, V.C.B., 2021. "Critical review on wax deposition in single-phase flow". *Fuel*, Vol. 293, pp. 1–20.

Venkatesan, R., 2004. *Deposition and Rheology of Organic Gels*. Ph.D. thesis, University of Michigan, Ann Arbor, MI.

White, F.M., 2011. *Fluid Mechanics*. Mechanical Engineering. McGraw-Hill.

Yang, J., Lu, Y., Daraboina, N. and Sarica, C., 2020. "Wax deposition mechanisms: Is the current description sufficient?" *Fuel*, Vol. 275, pp. 1–6.

7. Appendix

To proceed with the heat transfer calculations, the equation proposed by Davenport and Conti (1971) for the total heat transfer coefficient was applied and is represented in Eq.6 and was used to estimate the temperature distribution when the system reach the steady state condition.

$$\begin{aligned} U_{tot}A_{int}(T_{\infty oil} - T_{\infty water}) &= h_{oil}A_{int}(T_{\infty oil} - T_{int}) \\ = k_{deposit}\frac{2\pi L}{\ln\left(\frac{D_w}{D_{int}}\right)}(T_{int} - T_{wall_{in}}) &= k_{pipeline}\frac{2\pi L}{\ln\left(\frac{D_o}{D_w}\right)}(T_{wall_{in}} - T_{wall_{out}}) \\ &\approx h_{water}A_{wall_{out}}(T_{wall_{out}} - T_{\infty water}) \end{aligned} \tag{6}$$

where $T_{wall_{out}}$ is the average temperature at the pipeline outside wall and $A_{wall_{out}}$ is the outside area of the pipeline wall.

Assuming that the length is a lot bigger than the diameter, thus the variation of the diameter in the area thought which heat is transferred is negligible, e.g. $A_{int} \approx A_{wall}$ meaning that for the heat transfer calculation all diameters are the same.

$$\begin{aligned} U_{tot}(\pi D_{int}L)(T_{\infty oil} - T_{\infty water}) &= h_{oil}(\pi D_{int}L)(T_{\infty oil} - T_{int}) \\ = k_{deposit}\frac{2\pi L}{\ln\left(\frac{D_w}{D_{int}}\right)}(T_{int} - T_{wall_{in}}) &= k_{pipeline}\frac{2\pi L}{\ln\left(\frac{D_o}{D_w}\right)}(T_{wall_{in}} - T_{wall_{out}}) \\ &\approx h_{water}(\pi D_{int}L)(T_{wall_{out}} - T_{\infty water}) \end{aligned} \tag{7}$$

To calculate the temperature at the internal wall and the temperature of the interface,

$$U_{tot}(T_{\infty oil} - T_{\infty water}) = h_{oil}(T_{\infty oil} - T_{int}) \longrightarrow T_{int} = T_{\infty oil} - \frac{U_{tot}}{h_{oil}}(T_{\infty oil} - T_{\infty water}) \tag{8}$$

$$U_{tot}(T_{\infty oil} - T_{\infty water}) = \frac{2k_{deposit}}{D_{int}\ln\left(\frac{D_w}{D_{int}}\right)}(T_{int} - T_{wall_{in}}) \longrightarrow T_{wall_{in}} = T_{int} - \frac{U_{tot}}{\frac{2k_{deposit}}{D_{int}\ln\left(\frac{D_w}{D_{int}}\right)}}(T_{\infty oil} - T_{\infty water}) \tag{9}$$